The International Journal of Advanced Manufacturing Technology

Equal Channel Angular Sheet Extrusion (ECASE) as a precursor of heterogeneity in an AA6063-T6 alloy

--Manuscript Draft--

Manuscript Number:	JAMT-D-18-04605
Full Title:	Equal Channel Angular Sheet Extrusion (ECASE) as a precursor of heterogeneity in an AA6063-T6 alloy
Article Type:	Original Research
Keywords:	Aluminum alloy; Strain; Tensile test; Texture; EBSD; Dislocations; X-ray.
Corresponding Author:	Jairo Alberto Muñoz Universidad Nacional de Rosario Rosario, Santa Fe ARGENTINA
Corresponding Author Secondary Information:	
Corresponding Author's Institution:	Universidad Nacional de Rosario
Corresponding Author's Secondary Institution:	
First Author:	Jairo Alberto Muñoz
First Author Secondary Information:	
Order of Authors:	Jairo Alberto Muñoz
	Oscar Fabián Higuera
	Vanina Tartalini
	Pablo Risso
	Martina Avalos
	Raúl E. Bolmaro
Order of Authors Secondary Information:	
Funding Information:	Consejo Nacional de Investigaciones Científicas y Técnicas (CONICET D 4263) — Dr Jairo Alberto Muñoz
Abstract:	We study the deformation inducing heterogeneity in an Aluminum alloy 6063-T6 in the form of a sheet processed at room temperature by Equal Channel Angular Sheet Extrusion (ECASE) up to a maximum equivalent strain of 1.86 following route C. The through thickness strain distribution showed higher strains in the edge vicinities than in the sheet core. The texture was heterogeneous between the edges and the sheet core with a strong Cube component in the initial deformation stages, and a rolling texture with the S component in the sheet edges. Different microstructural characteristic, like grain size, average misorientation and fraction of High Angle Grain Boundaries (HAGB) decreased by increasing the deformation. The Geometrically Necessary Dislocation (GND) calculations corroborated the existence of a heterogeneous microstructure along the sheet thickness, giving rise to gradients of plastic deformation which allowed to obtain a good strength-ductility relationship. It was demonstrated that ECASE process was a good alternative to produce heterogeneous microstructures. The material heterogeneity was found not to be randomly distributed across the sheet thickness but rather showing higher dislocation concentration and bigger grain size reductions in the edge's vicinities than in its middle zone.
Suggested Reviewers:	Mahmood Fatemi University of Tehran mfatemi@ut.ac.ir Dr Fatemi knows quite well the mechanical behavior of light alloys under plastic deformation conditions.

	Francisco Cruz-Gandarilla Instituto Politecnico Nacional Escuela Superior de Fisica y Matematicas fcruz@ipn.mx Dr Cruz-Gandarilla has a lot of experience with the metallic materials characterization by EBSD.
	Heinz-Günter Brokmeier Technische Universitat Clausthal heinz-guenter.brokmeier@tu-clausthal.de Dr Brokmeier is an expert in texture characterization of metallic materials by X-ray diffraction.
	José María Cabrera Marrero Universitat Politecnica de Catalunya jose.maria.cabrera@upc.edu Professor Cabrera has been working with severe plastic deformation of metallic materials for the last ten years.

Dr. Jairo Alberto Muñoz Bolaños
Instituto Física de Rosario, Universidad Nacional de Rosario, Bv. 27 de Febrero, S2000EKF Rosario, Santa Fe, Argentina.
E-mail: jairomunoz8614@gmail.com
Tel.: +543415884754

Prof. Dr. David W. Russell
Editor-in-chief of the International Journal of Advanced Manufacturing Technology
November 21, 2018

Dear Professor,

Please find in attached files of our manuscript entitled **" Equal Channel Angular Sheet Extrusion (ECASE) as a precursor of heterogeneity in an AA6063-T6 alloy "** to be submitted electronically for publication in the International Journal of Advanced Manufacturing Technology. The manuscript has not been published before and is not currently submitted for publication to any other journal and will not be submitted elsewhere before a decision is made by this journal. This research work has been revised and approved by all the co-authors and institutions.

1. What is your main contribution to the field?

The relevance of this work to the materials science field is the capacity of a process which can be easily adapted to the industrial level to produce massive plane materials with a mix of hard and soft regions (i.e. a heterogeneous material).

2. What is novel? In theory, in experimental techniques, or a combination of both?

In our manuscript we are characterizing and showing the capability of ECASE process to produce heterogenous microstructures applied to sheet materials. The importance of a heterogeneous microstructure is coming from the fact that it can be a good option to produce materials with the presence of soft and hard regions, simultaneously. The current approach explores the possibility of inducing heterogeneity according to two different meanings: heterogeneous grain sizes and heterogeneous spatial distribution of those different grain sizes and it is explained by the strain, dislocations distribution and texture evolution. For that reason, the novelty with respect to experimental techniques is the full microstructure characterization along the sheet thickness as well as the insitu strain measurements by the digital image correlation technique.

3. Does your paper have industrial applications? If yes, who are the likely user?

We certainly believe it has industrial applications. The point is that in the past this technique was mainly devoted to introducing large amounts of deformation to produce nanostructure materials. But now, we are showing it has the capability to generate heterogeneous materials too by controlling the amount of deformation introduced in each material. We are still investigating the optimum conditions (amount of deformation) to get the desired heterogeneity. So, we think that the sheet metal forming industry could take advantage of this technique.

Waiting for your answer.

Yours sincerely

Dr. Jairo Alberto Muñoz Bolaños

Corresponding author
On behalf of all authors.

Equal Channel Angular Sheet Extrusion (ECASE) as a precursor of heterogeneity in an AA6063-T6 alloy

Jairo Alberto Muñoz[1, a, *], Oscar Fabián Higuera[2, b], Vanina Tartalini[1, c], Pablo Risso[1, d], Martina Avalos[1, e], Raúl E. Bolmaro[1, f].

[1]Instituto de Física Rosario, Consejo Nacional de Investigaciones Científicas y Técnicas-CONICET, Universidad Nacional de Rosario, Ocampo y Esmeralda, 2000 Rosario, Argentina
[2]Faculty of Engineering, Mechanical Engineering Program, Universidad del Atlántico, Barranquilla, Colombia

*Corresponding author: munoz@ifir-conicet.gov.ar

[a]munoz@ifir-conicet.gov.ar, [b]oscarhiguera@mail.uniatlantico.edu.co, [c]tartalini@ifir-conicet.gov.ar, [d]risso@ifir-conicet.gov.ar, [e]avalos@ifir-conicet.gov.ar, [f]bolmaro@ifir-conicet.gov.ar.

Abstract

We study the deformation inducing heterogeneity in an Aluminum alloy 6063-T6 in the form of a sheet processed at room temperature by Equal Channel Angular Sheet Extrusion (ECASE) up to a maximum equivalent strain of 1.86 following route C. The through thickness strain distribution showed higher strains in the edge vicinities than in the sheet core. The texture was heterogeneous between the edges and the sheet core with a strong Cube component in the initial deformation stages, and a rolling texture with the S component in the sheet edges. Different microstructural characteristic, like grain size, average misorientation and fraction of High Angle Grain Boundaries (HAGB) decreased by increasing the deformation. The Geometrically Necessary Dislocation (GND) calculations corroborated the existence of a heterogeneous microstructure along the sheet thickness, giving rise to gradients of plastic deformation which allowed to obtain a good strength-ductility relationship. It was demonstrated that ECASE process was a good alternative to produce heterogeneous microstructures. The material heterogeneity was found not to be randomly distributed across the sheet thickness but rather showing higher dislocation concentration and bigger grain size reductions in the edge's vicinities than in its middle zone.

Keywords: *Aluminum alloy, Strain, Tensile test, Texture, EBSD, Dislocations, X-ray.*

1 Introduction

Ultra-Fine Grain Materials (UFGM) via Severe Plastic Deformation (SPD), have been at the cutting edge of the material science for quite a while. Materials processed by SPD techniques present interesting behaviors, not only because of the free porosity of the material but also for the mechanical

properties. However, SPD leads to an increase in the strength while simultaneously reducing the homogeneous deformation zone because of reduction of strain hardening capacity leading to lower ductility [1, 2]. Another issue related with the production of UFGM is the low amount of high-quality material produced by SPD techniques, since the processing requirements (pressure, friction, and processing tool strength) highly increase with the processed material volume.

Some new SPD techniques based on the original principles of shear strain have been proposed for solving this problem. Equal Channel Angular Rolling (ECAR) [3] and Equal Channel Angular Sheet Extrusion (ECASE) [4] are some of these Equal Channel Angular Pressing (ECAP) modified techniques allowing the production of large ultrafine microstructure sheets. Besides, processes like ECASE and asymmetrical rolling (ASR) present an interesting characteristic, which is the possibility of a heterogeneous strain distribution in the material thickness. The aforementioned alternative can be a good choice to produce heterogeneous microstructures, which is a new option to obtain materials with good strength and ductility [5, 6].

In the ECASE process the true plastic strain is a function of simple shear per pass (γ), strain related with the elongation (ε_y) and thickness reduction (ε_x) components as given by [4]:

$$\varepsilon = \frac{\sqrt{2}}{3}\left[\left(\varepsilon_x - \varepsilon_y\right)^2 + \left(\varepsilon_x\right)^2 + \left(\varepsilon_y\right)^2 + \frac{3}{2}\gamma^2\right]^{1/2} \approx \frac{\gamma}{\sqrt{3}}\left[1 + 2\left(\frac{\varepsilon_y}{\gamma}\right)^2\right] \quad (1)$$

Where $\gamma = 2\tan\left(90° - \phi/2\right)$ and $\phi = 150°$, for the current experiments. In this way, the effective strain per ECASE pass can be estimated as ~0.31 and the true strain rate of the process can be calculated from [4]:

$$\dot{\varepsilon} = \varepsilon\vartheta/t \quad (2)$$

with ϑ as the drawing speed and t the sheet thickness.

The field of heterogeneous or gradient materials has drawn the attention of the research community over the last two years as a new alternative to produce metallic materials by plastic deformation keeping a good strength-ductility relationship [7, 8, 9]. In a heterogeneous structure both soft and hard regions can exist together, where it is expected that the soft regions support more the plastic deformation than hard ones, giving rise to gradients of plastic deformation [6]. In this way, the accommodation of such plastic gradients, requires the efficient storage of geometrically necessary dislocations [10]. For that reason, heterogeneous nanostructures are characterized by unusually small

length scale of gradient plastic deformation, and thus, offer a high capacity for storing more geometrically necessary dislocations, thereby enhancing the strain hardening and consequently a good combination of strength and ductility [7, 8].

The 6XXX family of Aluminum alloys are used in a variety of structural applications ranging from building and automotive to aerospace industries [11]. These alloys are among the most used aluminum alloys due to their attractive combination of mechanical properties, corrosion resistance, extrudability and excellent response to the surface finishing operations. Nowadays there are many studies concerning Al-Mg-Si alloys after deformation by ECAP and other SPD techniques [12, 13, 14, 15] . In most of them, the SPD process is carried out at moderate temperatures above ambient temperature [1, 16] to overcome the hardening effect of precipitates [17, 18, 19]. However, from the perspective of industrial applications, deformation at room temperature is much more convenient. Besides, there are not many studies of materials processed by ECASE at room temperature and its possibility to produce heterogeneous microstructures.

The concept of heterogeneity in the microstructure can be described in different ways, either as a mixture of large and small grains uniformly distributed throughout the material, or by the distribution of small and large grains in a non-random manner. In the last one, there are clearly identified regions where small and large grains are concentrated separately. The aim of this work is the study of the material heterogeneity induced by the ECASE process at room temperature and its effect over the mechanical properties, strain path, microstructure and texture evolution. In this way, the obtention of bulk severely deformed material was not the final goal of this study, since we were focused in investigating the effectiveness of its first stages to generate heterogeneity in the material.

The relevance of this work to the materials science field can be understood because of the possible capacity of the process of being easily adapted to industrial scales to produce large amounts of sheet materials with hard surfaces while keeping a soft core.

2 Experimental procedure

An Aluminum alloy 6063-T6 (0.35%Fe; 0.2-0.6%Si; 0.1%Mn; 0.45-0.9%Mg; 0.1%Cr; 0.1%Zn; 0.1%Ti; 0.1%Cu; Al (in wt %)) was received in the form of sheets of 38 mm width and 3.5 mm thickness. Before the ECASE process the material was heat treated at 530 °C for 4 hours and further water quenched, followed by heating at 190 °C for 10 hours and air cooling. The sheets were divided into billets having lengths of ~300mm, and these billets were subject to deformation by ECASE at room temperature. ECASE was carried out using a two parts die with an inner angle of $\Phi = 150^{o}$ (see Figure 1a), resulting in a true strain of ~0.31 per pass according with Zisman et al. [4]. Molybdenum

bisulfate (MoS_2) was used as a lubricant to minimize the friction effects between the die and the workpiece. 1.8 mm/min drawing speed was used for the ECASE process. Therefore, the true strain rate calculated with equation (2) was $2\times10^{-3}s^{-1}$.

To characterize the microstructure and texture evolution during the ECASE process, complete EBSD scans were performed in the TD plane through the complete sheet thickness, together with X-ray analysis. The microstructures of the samples were characterized by Electron Backscattered Diffraction (EBSD). For this purpose, specimens were cut from the TD plane of the ECASE samples (see Figure 1b) and were mechanically polished from 2500 grit SiC paper until 0.02 μm colloidal silica suspension, following standard metallographic procedures. Kikuchi patterns were acquired by using a TSL EDAX system mounted on a FEG-SEM (Quanta 200 - FEI). The data was processed with TSL OIM 7.3b software. The data processing parameters for OIM software were: maximum misorientation threshold angle of 5° for grain size calculation and clean-up subroutine by grain dilation with a minimum grain size of 4 points. To characterize the local texture, five EBSD maps were obtained with 1 μm step size covering the full sheet thickness. Detailed maps were analyzed with 0.2 μm step size in three different zones along the sheet thickness. Misorientations lower than 0.5° were not considered in the data post-processing. The orientation distribution functions (ODFs) were calculated by series expansion method using truncation at L=22 [20, 21].

The X-ray diffraction measurements of the processed samples were carried out on a Philips X pert Pro MPD diffractometer with Cu-Kα (1.5405Å) radiation, X-ray lenses, parallel plate collimator and Xe detector. The array was the one known as Schull reflection method [22, 23]. The specimens were mechanically polished to 1000 grit and then etched with Kellers solution (Figure 1b). The initial three measured pole figures were corrected for defocusing and further analyzed by WXpopLA [24] and MTEX [25] tool box.

Tension tests at room temperature at a constant strain rate of 1×10^{-3} s^{-1} were performed using an Instron 3362 universal testing machine. The specimens were machined out of the 3.5 mm thickness sheets (gauge dimension of 12 mm ×3 mm ×3.5 mm) by means of wire electrical discharge machining. The strength of the processed material was characterized by hardness measurements in the Knoop scale. Three different hardness profiles were measured for each ECASE pass along the sheet thickness to evaluate the hardening gradient between the zones closer to the edges and the sheet core.

To study the deformation introduced through the ECASE process, the free software Ncorr [26] and the commercial FEM software Abaqus were used (see Figure 1c). With Ncorr software, basically the

distribution of the deformation is obtained by Digital Image Correlation (DIC) [27] applied to a random pattern of black spots over a white color surface in the TD plane before and after the deformation process. For the sample preparation the surface of interest must be totally clean. After that, an initial layer of white paint was applied, followed by a layer of black paint spots. During the deformation test, pictures were taken every two seconds. In that way, the deformation was obtained by the comparison of the change in the black spots shape and position in an area before and after deformation (see Figure 1d).

For the FEM simulations some considerations were made. The material was considered isotropic and homogeneous, the system was isothermal at room temperature (T=20°C) and the heating conditions from the friction between the die and the workpiece were neglected. The parameters for describing the mechanical properties of the material were determined from the tensile test. The curve with strain beyond the maximum stress was extended as being ideally plastic following a Hollomon equation [28]. Since the deformations of the die are very small and they have very little effect on the stress-state of the specimen, the die was defined as discrete rigid and completely constrained as a rigid body. Considering the small width spread of the sheets, the deformation during the ECASE process was treated as a plane-strain model.

3 Results and discussion

3.1 Starting material

In Figure 2 the initial microstructures before and after the aging treatment are observed. The alloy in the solid solution state presents an equiaxed average grain size of 38 µm. Besides, the absence of the precipitation effect is also remarkable in this state. After the aging treatment a great number of particles appear inside of some grains, what can be attributed to the precipitation effect [29, 30, 31].

Figure 2 shows a high concentration of Mg in some grains and in the grain boundaries because of the aging heat treatment. Khelfa et al. [29] and Gavgali et al. [32] indicated that during quenching, the Mg–Si elements can be retained in solution. Therefore, the Al phase would contain Mg–Si in a supersaturated solid solution at room temperature. Thus, in the temperature range of 180 °C - 220 °C a formation of solute rich clusters of Mg_2Si would be obtained. In Figure 2 the existence of some Mg and Si rich zones is confirmed by the EDS analysis.

For the Abaqus simulation the tensile behavior of the initial material was also calculated and fitted to a Hollomon equation [28]. The initial material showed a yield and a maximum stress of ~190 and 270MPa respectively, with an elongation to failure of ~19%.

3.2 Strain of the ECASE process and mechanical properties

Figure 3 shows the strain distribution (strain components in the X and Y axes and the shearing component) calculated by Ncorr and Abaqus for the first ECASE pass. It can be seen in Figures 3a and 3b that the results obtained with both analyses are quite similar. The strain component values are higher in the edges than in the center of the sheet, proving that the ECASE process can introduce a heterogeneous state of deformation in the material. In Figure 3b it was also corroborated by Abaqus that the material was undergoing higher shear strains in regions closer to the surface.

In Figure 3c it can be observed a comparison of the experimental sheet after the first ECASE pass and the simulation obtained with Abaqus. The simulation after the first pass presents good correlation with the experimental result reproducing well the deformation effect over the sheet. In this figure the simulation shows the equivalent plastic deformation with values ranging from 0.2 to ~0.3, which is not far away from the theoretical value predicted by Zisman et al. [4].

Figure 4 presents the thickness reduction, hardness evolution and the tensile test for the different ECASE passes. The thickness reduction in Figure 4a shows a continuous decrease as the number of ECASE passes increase. It is worth mentioning that all the thickness reduction was compensated by the sheet length (i.e. the sheet width stayed constant for all the ECASE passes). On the other hand, the hardness evolution in Figure 4b allowed seeing some differences between the hardness near to the edges and the core. Besides, it was also seen an overall hardness increase with number of ECASE passes.

After the first pass, it can be seen how the main hardness gains were obtained in regions closer to the edges instead of the sheet core, where the hardness is quite similar to the initial material (T6 condition). However, as the deformation continued the hardness values were getting more homogeneous along the material thickness, as in the study of Fandiño et al. [33] with a magnesium alloy. The lower hardness increase observed in this study can be mainly attributed to both the lower amount of deformation introduced with each ECASE pass and the initial state of the starting material (T6 condition), since it is well know that the main hardening contribution of this alloy is coming from the precipitation effect as has been indicated in other studies [34]. Nevertheless, these hardness measurements allowed to see the capacity of this process for the generation of hard and soft zones through the sheet thickness.

In Figure 4c the tensile curves at different number of ECASE passes are indicated. At first glance, it can be observed the increment in the yield stress for the processed materials with respect to the undeformed material. The increase in the maximum stress was not as remarkable as the values

obtained by techniques such as ECAP for the same alloy [35, 36]. However, in Figure 4d it can be seen how the strain hardening capacity with the ECASE process is less affected than with other SPD processes like ECAP [35, 36] or twist extrusion (TE) [37] for the same alloy, where the strain hardening region almost disappears once the yield stress was reached.

Figure 4d allows to see the strain hardening rate for both undeformed and deformed materials. The most deformed materials (i.e. three, four and six ECASE passes) presented a higher strain hardening rate at the initial stages of deformation. However, the extension of the strain hardening region in those materials is very small. On the other hand, after one ECASE pass it can be appreciated a bigger extension of the strain hardening zone with a strain hardening rate quite comparable to the undeformed material (0P). For the above, it can be inferred that the ECASE process produces materials with good strength and ductility, since it has been stablished by Valiev et al. [38] that strain hardening is the primary approach for improving ductility due to the most effective accumulation of dislocations.

3.3 Microstructure and texture

3.3.1 Texture evolution

Texture characterization was done following the evolution of the ideal rolling and simple shearing texture components and fibers for FCC materials described in Figure S1, Table S1 and Table S2 from the supplementary material. The EBSD scans and the X-ray results can be seen in Figure 5 to Figure 7. Local texture analysis (EBSD) were done in three areas, one in the surroundings of the inner edge, the second in the sheet core and the third in the surroundings of the outer edge.

In Figure 5 the EBSD measurements for the initial materials in the solid solution and after the aging treatment did not show remarkable texture differences between them. However, texture differences between the edges and the core were found. Strong components, such as Cube, Goss and Brass were dominant in the sheet core, while in the edges, the Cube, Goss, S, Brass and Dillamore components, although dominating the texture (see Figure 8), showed a lower intensity. For that reason, the overall texture measurements from X-ray diffraction allowed to see that the dominant texture corresponds well with a strong Cube component. Some researchers [39, 40, 41] have suggested that this behavior can be associated with a recrystallization texture.

In materials with one and two ECASE passes texture differences were observed between the edges and the core. After one pass, in the sheet core zone, the Cube and Goss components appear with more intensity than the others, but with a lower volume fraction than the initial condition (Figure 8b). On the other hand, The S component appears as the most important in the inner and outer edges (see

Figure 6 and Figure 8). While, the overall texture measurement by X-ray highlights the Cube, Goss and S components as the most representative (see Figure 8d).

With two ECASE passes the texture intensity (local and overall) decreases in comparison with one ECASE pass material. However, edge's texture showed the S component as the strongest along the sheet thickness followed by the Dillamore and Brass components in the inner and outer edges, respectively. According with the research work of Naseri et al. [42] for an AA2024 alloy processed by Accumulative Roll Bonding (ARB), the surge of these components is more characteristic of a rolled material. In the case of the sheet core, Figure 8b shows the emergence of the Y component as the main rolling texture contribution, although its volume fraction was lower than the S component, giving rise to an overall texture dominated by the S component.

After four and six ECASE passes, the overall texture severity continues decreasing. Even when, the local measurements allow seeing higher intensities in the edges than in the sheet core, especially after four passes. The X-ray texture measurement for the material with four passes shows the S component as the most important followed by the Cube, Goss, Dillamore, Brass and copper components. Meanwhile, the EBSD measurements indicated that the presence of strong S and Goss components was mainly coming from the edges and not from the center, where just a 5% volume fraction of the Y component draws attention, what leads to a texture dominated by the edge components. The appearance of the Y component is a consequence of shear banding occurring in the Y orientation [39]. Those shear bands can consist of very small elongated crystallites that are separated by High Angle Grain Boundaries (HAGB), which is coherent with the microstructure evolution showed in Figures 6 and 7, where it can be observed an increasing fraction of sub-grains inside of the elongated grains.

In the material with six passes some texture differences between the three zones were still seen with a higher volume fraction of the S component in the middle zone and a less representative volume fraction of the E, Y and rotated Copper components in the edges. It is worth mentioning that at this deformation it was obtained the lowest volume fractions of rolling texture components (Cube, Goss, Brass, Copper and S), together with the most important contribution in the shear components (rotated Cube, rotated Copper, E and Y components) associated with the rolling process.

Analyzing the overall rolling texture measurements (Figure 8d) it was observed that the volume fractions of the Cube and Goss components decrease proportionally with the deformation. Conversely, components like S, Brass, Dillamore and copper did not show significate changes in their volume fractions at different number of ECASE passes. On the other hand, the components in the

rolling plane associated with shearing (Rotated Cube, rotated Copper, E and Y) presented slight strengthening with the deformation increments.

In Figure 9 are indicated the volume fraction of the simple shear components obtained following the methodology described by other authors [43, 44]. At first glance, the existence of these components was mainly found in the zones close to the edges, and their intensities were lower than most of the components calculated in the rolling plane. The X-ray results showed that the material with one pass presented the highest volume fractions in almost all the simple shear components with respect to the other ECASE passes. In Figure 9b it can be also noted the almost none existence of simple shear components in the sheet core.

Analyzing the edge zones (Figures 9a and 9c) it can be observed that after one pass the component A_1^* was the more intense, whereas after two passes the C and B components, located in the inner and outer edges respectively, were the most representative. With four passes, the C component appeared as the most intense and it was mainly found around the edges. Besides, with six passes the main contributions were coming from the A and $\bar{A}$ components. For the first four passes the EBSD measurements allowed also to see the presence of the partial <110> fiber (A, $\bar{A}$, B, $\bar{B}$ and C) in the two edge zones. In the case of the material with six passes a partial <110> fiber was also found but with a high-volume fraction of the A and $\bar{A}$ components.

The pole figures in Figures 6 and 7 clearly show a rotation in the anticlockwise or the clockwise direction as the number of ECASE passes increases. The overall texture highlights a shift of ~ 15°, -7°, 7° and 7° for the processed materials around the TD axe. This texture change can be attributed to the shearing effect of these SPD techniques based on the shear strain, such as ECAP [45, 46]. However, the local measurements did not show a texture twist of that magnitude, following the simple shear texture components.

The strengthening and weakening of some texture components as well as the overall texture intensity can be attributed to the fact that the correct interpretation of the measured textures requires the dynamic overlap of the correct velocity gradients, according to the already known phenomena of extra spin contribution to the texture development [47]. The net effects are the rotation of some components, smearing out of some others and general decrease of the texture strength because of the non-stationary material flux during shearing.

In summary, it can be inferred that the ECASE process induce textures with well-defined strong components. According with some researchers [48, 49] the development of textures with sharp components leads to the formation of a band-like structure and prevents the full grain refinement to

a submicron scale. The mixture of different texture components in this process is a consequence of the combination of monotonic (rolling) and not monotonic (shearing) deformations which was confirmed by Ncorr and Abaqus calculations. It has been demonstrated by Bobor et al. [50] that shearing can be considered as a not monotonic process which can lead not only to texture changes but also to microstructure modifications. This is coherent with other investigations in processes like rolling and asymmetrical rolling [51, 52], where it was found the existence of shearing components in the edge vicinities while the rolling components were more intense in the sheet core.

3.3.2 Microstructure characterization

In Table 1 are summarized the grain size, HAGB fractions and average misorientation values for the three analyzed zones after different ECASE passes. The initial microstructure (0 passes) is mainly formed by equiaxed grains formed by HAGB in the edges and LAGB in the sheet core (see Figure 5 and Table 1). With the first ECASE pass the grain size decreases in the three regions, especially in the edges. That could be associated with the high strains generated in those zones as the Ncorr and Abaqus calculations already indicated. After two ECASE passes, one can observe a more strained microstructure, having a large fraction of low angle grain boundaries (LAGB) together with a smaller grain size.

With four passes, an extra reduction in the grain size has been reached with values ranging between 8 μm and 15 μm. On the other hand, in the material with six passes (Figure 7) a more pronounced microstructure change can be seen, where some small grains start to appear next to still bigger original grains. Those microstructure changes can be associated with the occurrence of Continuous Dynamic Recrystallization (CDRX) as it can be confirmed in Table 1 by the increments observed in the HAGB fraction and average misorientation. In Table 1 it is also evident that the initially observed differences in grain size, HAGB fraction and average misorientation between edges and center are reduced due to the more homogeneous strain distribution through the material thickness.

Therefore, the evolution in the HAGB fraction with the deformation is a consequence of the continuous transformation of LAGB from initial stages of deformation evolving to geometrically necessary boundaries which are formed and then subdivide the coarse grains into cell blocks [53]. For that reason, after the first four passes, a high fraction of LAGB was identified, while in subsequent passes those LAGB evolved into HAGB by adsorption of dislocations increasing the orientation differences between grain boundaries, as it is confirmed in Table 1 with the increments in the average misorientation values.

Geometrically Necessary Dislocations (GND)

The density of Geometrically Necessary Dislocations (GNDs) can be calculated from EBSD data [54, 55]. Figure 10 shows GND density maps for both initial and deformed samples in the inner edge region. The initial condition does not exhibit GNDs grouping. Over the scanned area they look quite homogeneously distributed with an average value of $3.1 \cdot 10^{12}\ m^{-2}$, a maximum of $1.3 \cdot 10^{13}\ m^{-2}$ and an average in the edge neighborhood of $3.1 \cdot 10^{12}\ m^{-2}$ (red dashed line rectangle).

After one pass some GND grouping are observed close to the edge, where the overall average value was $7.8 \cdot 10^{12}\ m^{-2}$, with a maximum value of $4.7 \cdot 10^{13}\ m^{-2}$ while the average close to the edge was of $1.2 \cdot 10^{13}\ m^{-2}$ (see the GND map and the peak shift in Figure 10). With two ECASE passes a more pronounced GND increment close to the sheet edge was observed with a value of $3 \cdot 10^{13}\ m^{-2}$, an overall average of $2.6 \cdot 10^{13}\ m^{-2}$ and a maximum value of $7.2 \cdot 10^{13}\ m^{-2}$.

As in the material with two passes, the material after four passes also shows a high GND density in the edge surroundings with a value of $3.7 \cdot 10^{13}\ m^{-2}$, an overall average value of $2.7 \cdot 10^{13}\ m^{-2}$ and a maximum of $2 \cdot 10^{14}\ m^{-2}$. Conversely, the material with six ECASE passes did not show any noticeable dislocation density difference between the edge surroundings and farther areas. In this case, the overall average and the average close to edge were $3.5 \cdot 10^{13}\ m^{-2}$ and $3.3 \cdot 10^{13}\ m^{-2}$, respectively, with a maximum of $2.4 \cdot 10^{14}\ m^{-2}$.

The GND evolution showed an increasing behavior with the deformation. Besides, with the GND analysis we can observe that the differences between the edges and the sheet core disappear after six ECASE passes due to a higher deformation accumulation giving rise to a more homogeneous strain distribution in the sheet. However, these high-density values of GNDs close to the edges after one, two and four ECASE passes show that this technique can be a viable alternative to produce a heterogeneous microstructure with a mix of hard and soft zones in the material.

The high density of GNDs close to the edges not only confirmed the heterogeneity due to the ECASE process but also the capacity to obtain a material with good strength and ductility properties as was showed before with the tensile tests.

4 Conclusions

The ECASE process proved to be an effective tool to produce sheet materials with heterogeneous microstructure. It was found that the heterogeneity of the processed material was due to the state of deformation introduced by each ECASE pass, with greater shearing deformations in the areas near the edges than in the center of the sheet.

The heterogeneity effect was reflected in the texture analyses with a mixture of components related with rolling and shearing deformation processes distributed between the center and edge zones, respectively. In the same way, the microstructure was heterogeneous with different grain sizes and HAGB fractions between the sheet edges and its core.

The GND evolution confirmed the generation of regions of higher strength giving rise to gradients of plastic deformation confirming a heterogeneous microstructure with higher density of dislocations in the edges than in middle zone. The GND maps also indicated that for this alloy the gradient of plastic deformation was reduced with the increment in the amount of deformation because of strain accumulation and thickness reduction.

Acknowledgements: JAMB thanks the Latin-American Postdoctoral scholarship (Grant number CONICET D 4263) received from the Argentine Ministry of Science, Technology and Productive Innovation and the National Council of Scientific and Technical Research. (CONICET).

Conflicts of Interest: The authors declare not conflict of interest.

References

[1] R. Z. Valiev, I. V. Alexandrov, Y. T. Zhu and T. C. Lowe, "Paradox of Strength and Ductility in Metals Processed By severe Plastic Deformation," *JMR*, vol. 17, pp. 5-8, 2002.

[2] J. A. Muñoz, O. F. Higuera and J. M. Cabrera, "Microstructural and mechanical study in the plastic zone of ARMCO iron processed by ECAP," *Materials Science and Engineering: A*, vol. 697, pp. 24-36, 2017.

[3] J. Han, K. Oh and J. Lee, "Effect of accumulative strain on texture evolution in 1050 Al alloys processed by continuous confined strip shearing," *Mater. Sci. Eng. A*, vol. 387, pp. 240-243, 2004.

[4] A. Zisman, V. Rybin, S. Van Boxel , M. Seefeldt and B. Verlinden, " Equal channel angular drawing of aluminium sheet," *Materials Science and Engineering A*, vol. 427, pp. 123-129, 2006.

[5] Z. Zeng, X. Li, D. Xu, L. Lu, H. Gao and T. Zhu, "Gradient plasticity in gradient nano-grained metals," *Extreme Mechanics Letters*, vol. 8, pp. 213-219, 2016.

[6] E. Ma and T. Zhu, "Towards strength–ductility synergy through the design of heterogeneous nanostructures in metals," *Materials Today*, vol. 20, pp. 323-331, 2017.

[7] R. Kalsar and S. Suwas, "A novel way to enhance the strength of twinning induced plasticity (TWIP) steels," *Scripta Materialia*, vol. 154, pp. 207-211, 2018.

[8] F. Yin, G. J. Cheng, R. Xu, K. Zhao, Q. Li, J. Jian, S. Hu, S. Sun, L. An and Q. Han, "Ultrastrong nanocrystalline stainless steel and its Hall-Petch relationship in the nanoscale," *Scripta Materialia*, vol. 155, pp. 26-31, 2018.

[9] X. Liu, F. Yuan, Y. Zhu and X. Wu, "Extraordinary Bauschinger effect in gradient structured copper," *Scripta Materialia,* vol. 150, pp. 57-60, 2018.

[10] M. F. Ashby, "The deformation of plastically non-homogeneous materials," *Philos. Mag,* vol. 21, pp. 399-424, 1970.

[11] T. Sheppard, Extrusion of Aluminium Alloys, Springer Science & Business Media., 2013.

[12] C. Xu, Z. Horita and T. G. Langdon, "Microstructural evolution in an aluminum solid solution alloy processed by ECAP," *Mater Sci Eng A,* vol. 528, pp. 6059-6065, 2011.

[13] S. D. Terhune, D. L. Swisher, K. Oh-ishi, Z. Horita, T. G. Langdon and T. R. McNelley, "An investigation of microstructure and grain-boundary evolution during ECA pressing of pure aluminum," *Metall Mater Trans A,* vol. 33, pp. 2173-2184, 2002.

[14] W. J. Kim, Y. K. Sa, H. K. Kim and U. S. Yoon, "Plastic forming of the equal-channel angular pressing processed 6061 aluminum alloy," *Mater Sci Eng A,* vol. 487, pp. 360-368, 2008.

[15] A. Loucif, R. B. Figueiredo, T. Baudin, F. Brisset and T. G. Langdon, "Microstructural evolution in an Al-6061 alloy processed by high-pressure torsion," *Materials Science and Engineering A,* vol. 527, p. 4864–4869, 2010.

[16] R. Z. Valiev, N. A. Krasilnikov and N. K. Tsenev, "Plastic deformation of alloys with submicron-grained structure," *Mater Sci Eng A,* vol. 137, pp. 35-40, 1991.

[17] S. R. Claves, D. L. Elias and W. Z. Misiolek, "Analysis of the intermetallic phase transformation occurring during homogenization of 6XXX aluminum alloys,," *Mater Sci Forum,* vol. 396, pp. 667-674, 2002.

[18] S. Zajac , B. Hutchinson, A. Johansson and L. O. Gullman, "Microstructure control and extrudability of Al−Mg−Si alloys microalloyed with manganese," *Mat Sci Tech,* vol. 10, pp. 323-333, 1994.

[19] N. C. W. Kuijpers, W. H. Kool and S. Zwaag, "DSC study on Mg−Si phases in as-cast 6XXX," *Mater Sci Forum,* vol. 396, pp. 675-680, 2002.

[20] S. Suwas and R. K. Ray, Crystallographic Texture of Materials, London: Springer-Verlag, 2014.

[21] H. J. Bunge, "Fabric analysis by orientation distribution functions," *Tectonophysics,* vol. 78, pp. 1-21, 1981.

[22] L. G. Schulz, "A Direct Method of Determining Preferred Orientation of a Flat Reflection Sample Using a Geiger Counter X-Ray Spectrometer," *Journal of Applied Physics,* vol. 20, p. 1030, 1949.

[23] D. Chateigner, P. Germi and M. Pernet, "Texture Analysis by the Schulz Reflection Method: Defocalization Corrections for Thin Films," *J. Appl. Cryst,* vol. 25, pp. 766-769, 1992.

[24] J. S. Kallend, U. F. Kocks, A. D. Rollett and H. R. Wenk, "Operational texture analysis," *Mater. Sci. Eng. A,* vol. 132, pp. 1-11, 1991.

[25] F. Bachmann, R. Hielscher and H. Schaeben, "Texture Analysis with MTEX - Free and Open Source Software Toolbox," *Solid State Phenomena,* vol. 160, pp. 63-68, 2010.

[26] J. Blaber, B. Adair and A. Antoniou, "Ncorr: Open-Source 2D Digital Image Correlation Matlab Software," *Experimental Mechanics* , vol. 55, p. 1105–1122, 2015.

[27] A. F. Ab Ghani, M. B. Ali, S. DharMalingam and J. Mahmud, "Digital Image Correlation (DIC) Technique in Measuring Strain Using Opensource Platform Ncorr," *Journal of Advanced Research in Applied Mechanics,* vol. 26, pp. 10-21, 2016.

[28] J. H. Hollomon, "Tensile deformation," *Aime Trans,* vol. 12, pp. 1-22, 1945.

[29] T. Khelfa, M. A. Rekik, M. Khitouni and J. M. Cabrera-Marrero, "Structure and microstructure evolution of Al–Mg–Si alloy processed by equal-channel angular pressing," *Int J Adv Manuf Technol,* vol. 92, pp. 1731-1740, 2017.

[30] S. K. Panigrahi, R. Jayaganthan, V. Pancholi and M. Gupta, "A DSC study on the precipitation kinetics of cryorolled Al 6063 alloy," *Mater Chem Phys,* vol. 122, p. 188–193, 2010.

[31] R. S. Yassar , D. P. Field and H. Weiland, "The effect of cold deformation on the kinetics of the β″ precipitates in an Al-Mg-Si alloy," *Metall Mater Trans A,* vol. 36, p. 2059–2065, 2005.

[32] M. Gavgali, Y. Totik and R. Sadeler, "The effects of artificial aging on wear properties of AA 6063 alloy," *Materials Letters,* vol. 57, pp. 3713-3721, 2003.

[33] E. M. Fandiño, R. E. Bolmaro, P. Risso, V. Tartalini, P. F. Morales and M. Ávalos, "Microstructure, and Surface Mechanical Properties of AZ31 Magnesium Alloys Processed by ECASD," *Adv. Eng. Mater,* p. 1700228, 2017.

[34] T. Khelfa, M. A. Rekik, J. A. Muñoz-Bolaños, J. M. Cabrera-Marrero and M. Khitouni, "Microstructure and strengthening mechanisms in an Al-Mg-Si alloy processed by equal channel angular pressing (ECAP)," *Int J Adv Manuf Technol,* vol. 95, pp. 1165-1177, 2017.

[35] T. Qian, M. Marx, K. Schüler, M. Hockauf and H. Vehoff, "Plastic deformation mechanism of ultra-fine-grained AA6063 processed by equal-channel angular pressing," *Acta Materialia,* vol. 58, pp. 2112-2123, 2010.

[36] M. Samaee, S. Najafi, A. R. Eivani, H. R. Jafarian and J. Zhou, "Simultaneous improvements of the strength and ductility of fine-grained AA6063 alloy with increasing number of ECAP passes," *Materials Science and Engineering: A,* vol. 669, pp. 350-357, 2016.

[37] H. Zendehdel and A. Hassani, "Influence of twist extrusion process on microstructure and mechanical properties of 6063 aluminum alloy," *Materials & Design,* vol. 37, pp. 13-18, 2012.

[38] R. Z. Valiev, Y. Estrin, Z. Horita, T. G. Langdon, M. J. Zehetbauer and Y. T. Zhu, "Fundamentals of superior properties in bulk nanoSPD materials," *Materials Research Letters,* vol. 4, pp. 1-21, 2016.

[39] F. Humphreys and M. Hatherly, Recrystallization and related annealing phenomena, Oxford,United Kingdom: Pergamon, 1996.

[40] S. De La Chapelle and P. Duval, "Recrystallization in a hot deformed Al-Mg-Si alloy: T he effect of fine precipitates," *Textures and Microstructures,* vol. 35, pp. 55-70, 2002.

[41] O. Engler and V. Randle, IntroductiontoTextureAnalysis – Macrotexture,Microtexture, and Orientation Mapping, second ed ed., United States of America: Taylor&FrancisGroup, 2010.

[42] M. Naseri, M. Reihanian and E. Borhani, "A new strategy to simultaneous increase in the strength and ductility of AA2024Nalloy via accumulative roll bonding (ARB)," *Materials Science & Engineering A,* vol. 656, pp. 12-20, 2016.

[43] S. Li, I. J. Beyerlein and M. A. M. Bourke, "Texture formation during equal channel angular extrusion of fcc and bcc materials: comparison with simple shear," *Materials Science and Engineering: A,* vol. 394, pp. 66-77, 2005.

[44] G. R. Canova, U. F. Kocks and J. J. Jonas, "Theory of torsion texture development.," *Acta Metallurgica,* vol. 32, pp. 211-226, 1984.

[45] I. J. Beyerlein and L. S. Tóth, "Texture evolution in equal-channel angular extrusion," *Progress in Materials Science,* vol. 54, pp. 427-510, 2009.

[46] L. S. Tóth, "Texture Evolution in Severe Plastic Deformation by Equal Channel Angular Extrusion," *Adv. Eng. Mater,* vol. 5, p. 308–316, 2003.

[47] R. E. Bolmaro and U. F. Kocks, "A comparison of the texture development in pure and simple shear and during path changes," *Scripta METALLURGICA et MATERIALIA,* vol. 27, pp. 1717-1722, 1992.

[48] S. Pasebani, M. R. Toroghinejad, M. Hosseini and J. Szpunar, "Textural evolution of nano-grained 70/30 brass produced by accumulative roll-bonding," *Mater.Sci.Eng.A527 (2010),* vol. 527, p. 2050–2056, 2010.

[49] R. Jamaati and M. R. Toroghinejad, "Effect of alloy composition, stacking fault energy, second phase particles, initial thickness, and measurement position on deformation texture development of nanostructured FCC materials fabricated via accumulative roll bonding process," *Materials Science and Engineering: A,* vol. 598, pp. 77-97, 2014.

[50] K. Bobor and G. Krallics, "Characterization of severe plastic deformation techniques with respect to non-monotonity," *Rev. Adv. Mater. Sci,* vol. 25, pp. 32-41, 2010.

[51] H. Jin and D. J. Lloyd, "The different effects of asymmetric rolling and surface friction on formation of shear texture in aluminium alloy AA5754," *Mater. Sci. Technol,* vol. 26, 2009.

[52] H. K. Kim, H. W. Kim, J. H. Cho and J. C. Lee, "High-formability Al alloy sheet produced by asymmetric rolling of strip-cast sheet," *Mater. Sci. Eng. A.* , vol. 574, pp. 31-36, 2013.

[53] Y. Tomita and K. Okabayashi, "Tensile stress-strain analysis of cold worked metals and steels and dual-phase steels," *Metall. Trans. A,* vol. 16, p. 865, 1985.

[54] W. Pantleon, "Resolving the geometrically necessary dislocation content by conventional electron backscattering diffraction," *Scripta Materialia,* vol. 58, pp. 994-997, 2008.

[55] J. F. Nye, "Some geometrical relations in dislocated crystals," *Acta Metall,* vol. 1, pp. 153-162, 1953.

Figure captions

Figure 1. a) ECASE configuration, b) EBSD and XRD samples, c) Abaqus parameters, d) Ncorr parameters and e) tensile test initial material.
Figure 2. Initial material characterization.
Figure 3. Ncorr and Abaqus results, a) Ncorr strains after one ECASE pass, b) Abaqus strains after one ECASE pass and c) experimental and Abaqus simulation of the sheet after the first ECASE pass.
Figure 4. Mechanical properties of the AA6063T6 processed by ECASE a) Thickness reduction, b) hardness evolution, c) true stress-strain curves and d) strain hardening rate at different number of ECASE passes.
Figure 5. Texture (local and overall measurements) and microstructure characterization for the initial material (for the IPF color representation [001]∥TD).
Figure 6. Texture (local and overall measurements) and microstructure characterization for the material with 1 and 2 ECASE passes (for the IPF color representation [001]∥TD).
Figure 7. Texture (local and overall measurements) and microstructure characterization for the material with 4 and 6 ECASE passes (for the IPF color representation [001]∥TD).
Figure 8. Rolling texture components evolution for AA6063T6 at different points along the sheet thickness, a) Inner edge, b) center, c) outer edge and d) overall measurements by X-ray.
Figure 9. Shearing texture components evolution for AA6063T6 at different points along the sheet thickness, a) Inner edge, b) center, c) outer edge and d) overall measurements by X-ray.
Figure 10. GND maps for the unprocessed and processed AA6063-T6

Figure S1. Ideal texture components and fibers for FCC materials, a) simple shear components and b) rolling components.

Table captions

Table 1. Microstructure characteristics in the three zones.

Table S1. Ideal texture components for FCC materials.
Table S2. Simple shear texture components

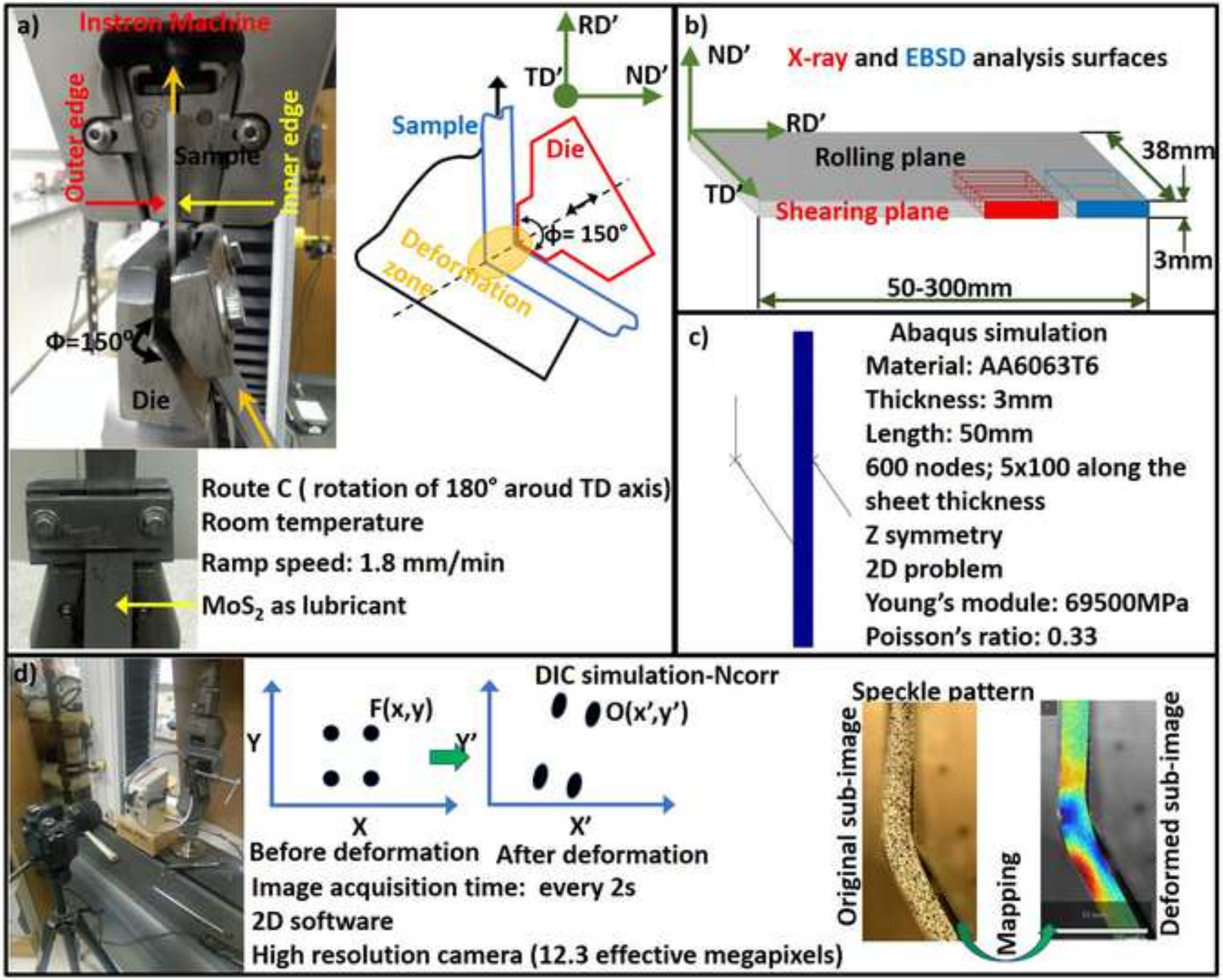

Figure2

Click here to download Figure Figure 2.jpg

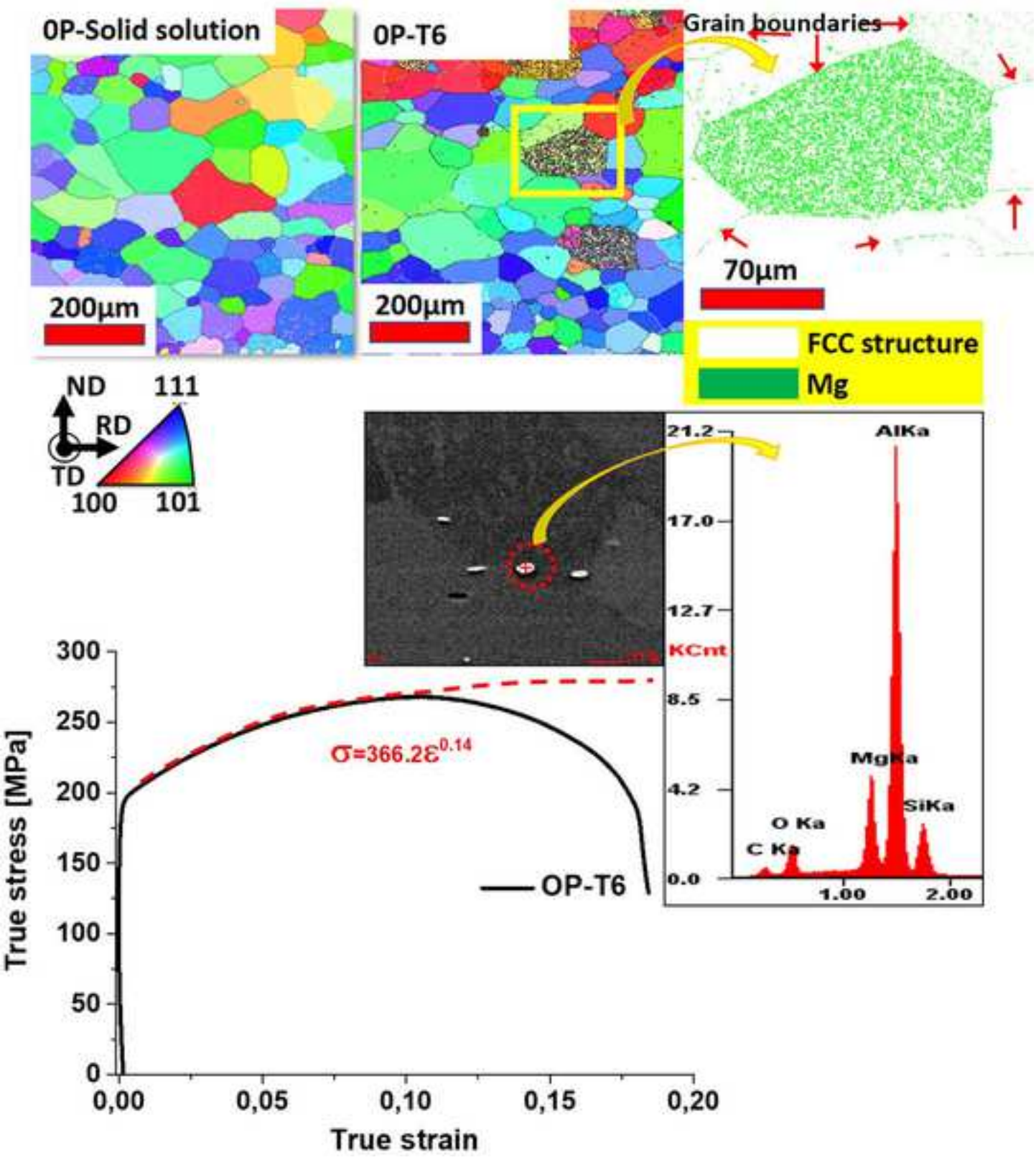

Figure3

Click here to download Figure Figure 3.jpg

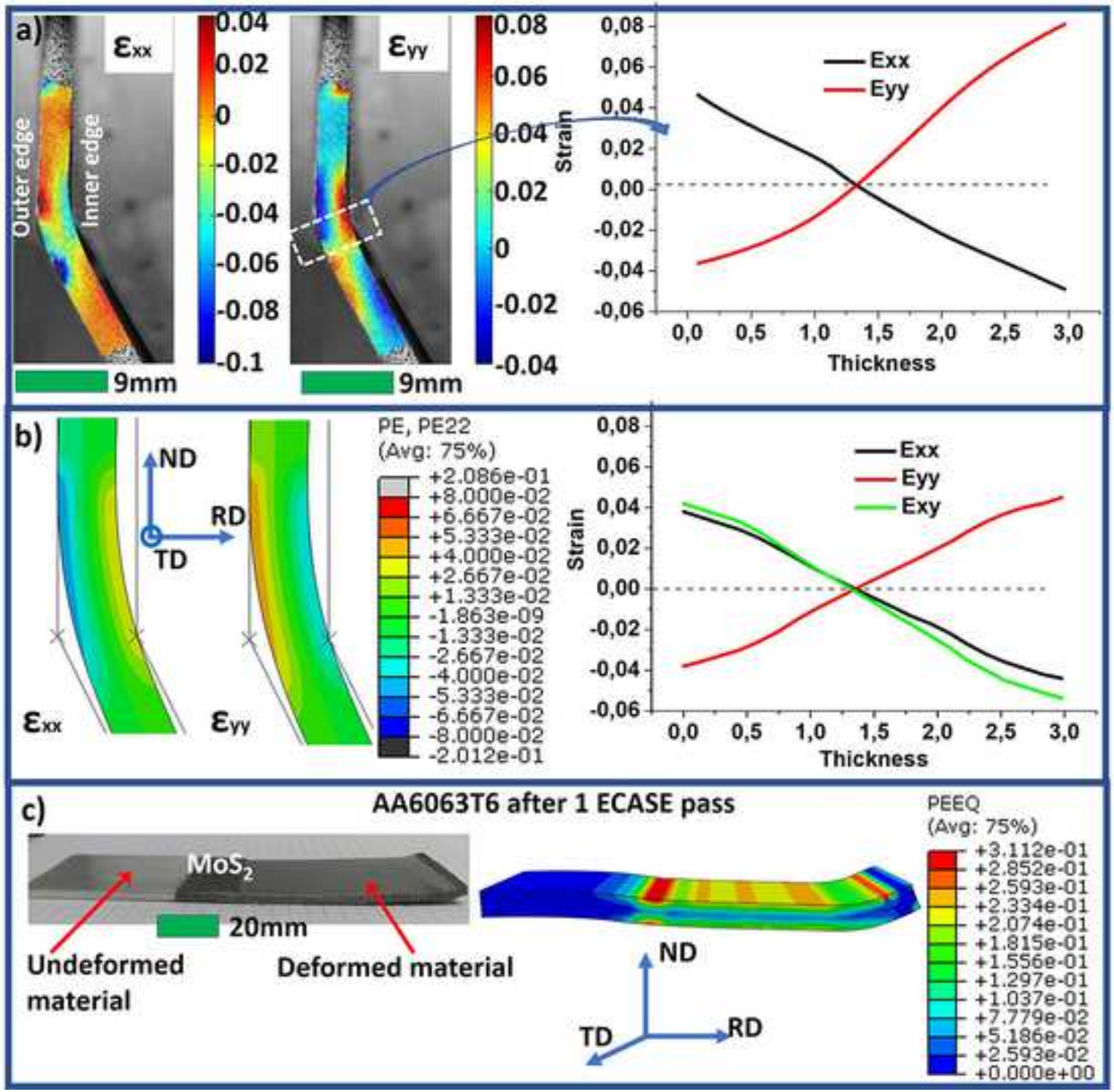

Figure4

Click here to download Figure Figure 4.jpg

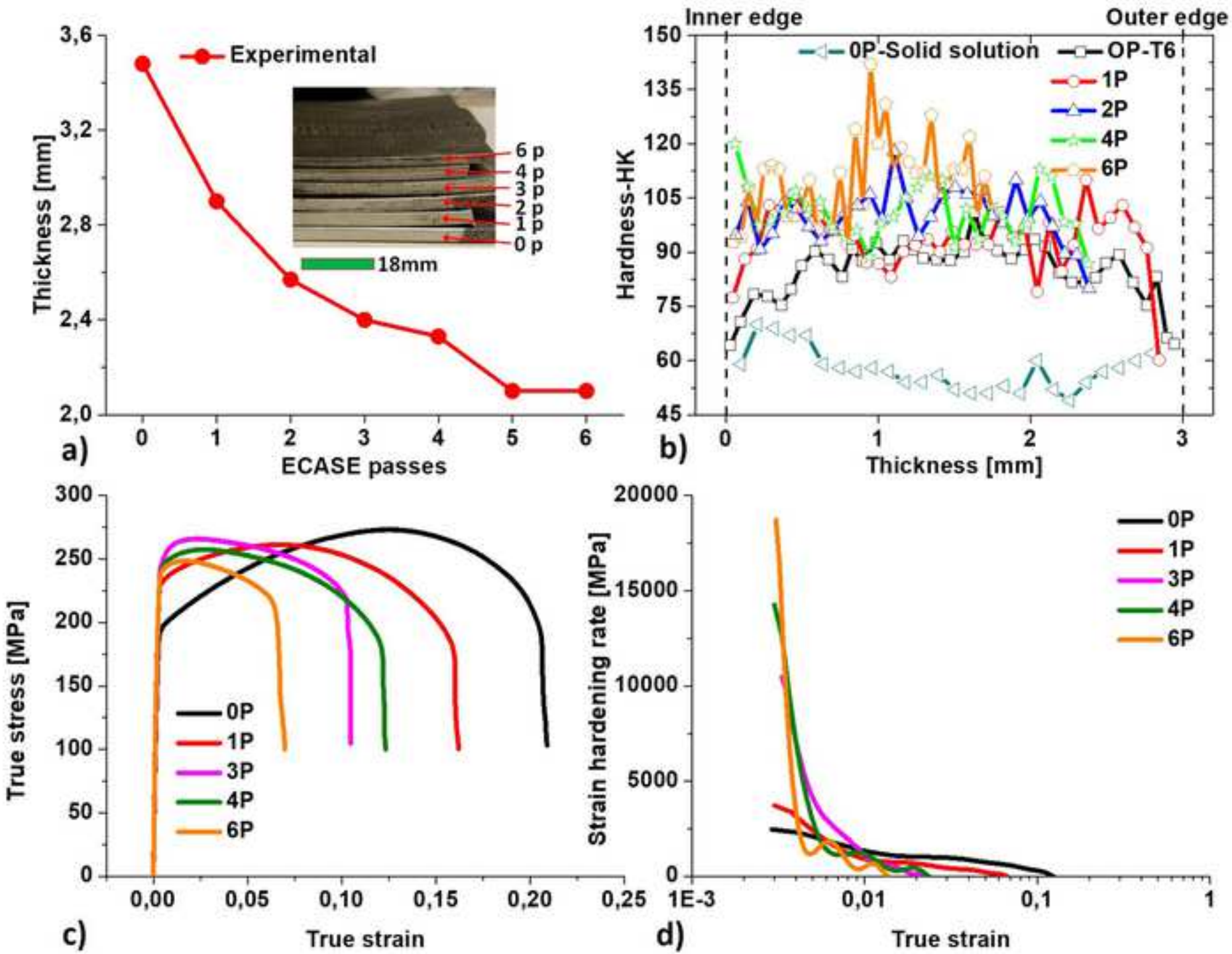

Figure5

Click here to download Figure Figure 5.jpg

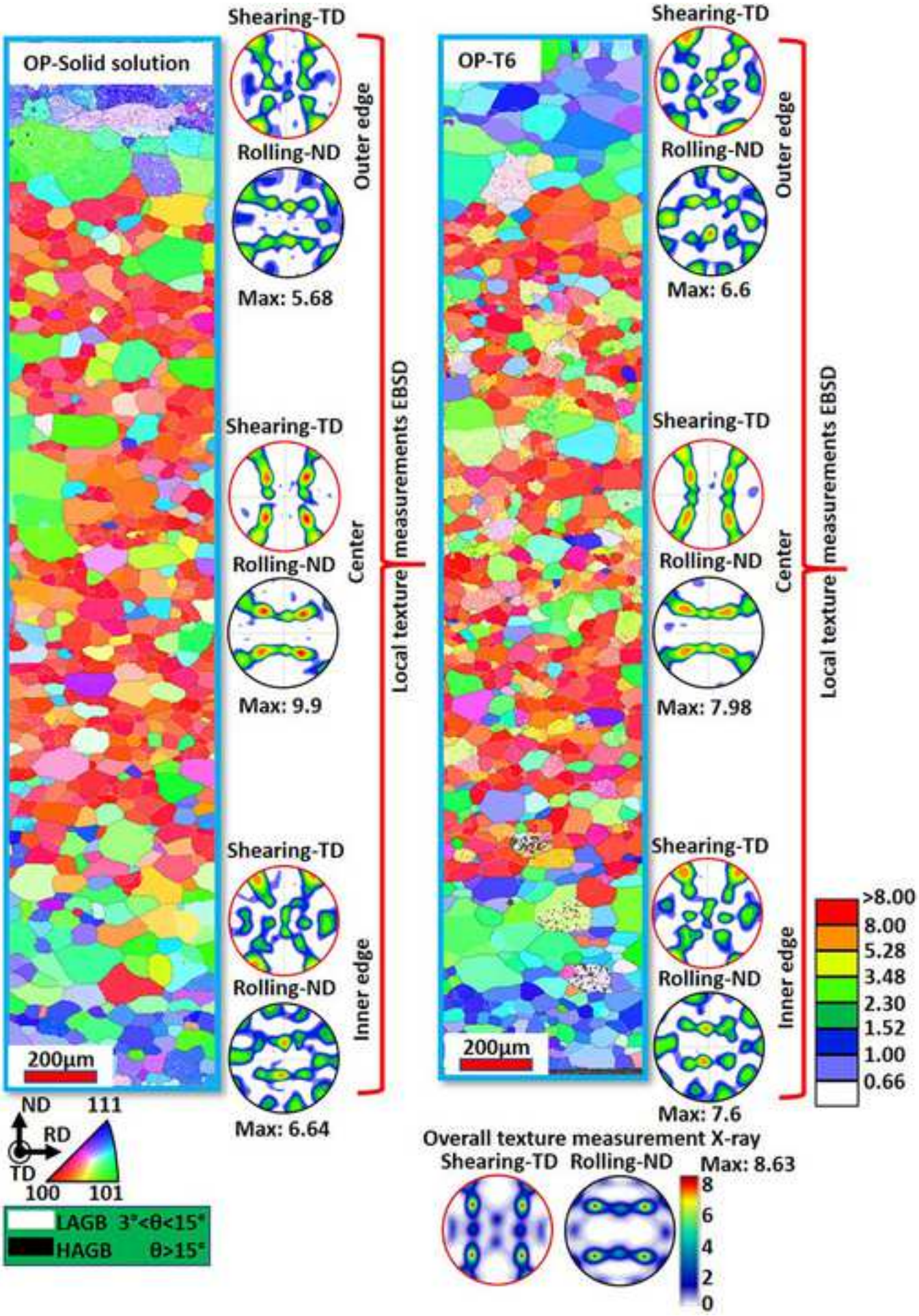

Figure6

Click here to download Figure Figure 6.jpg

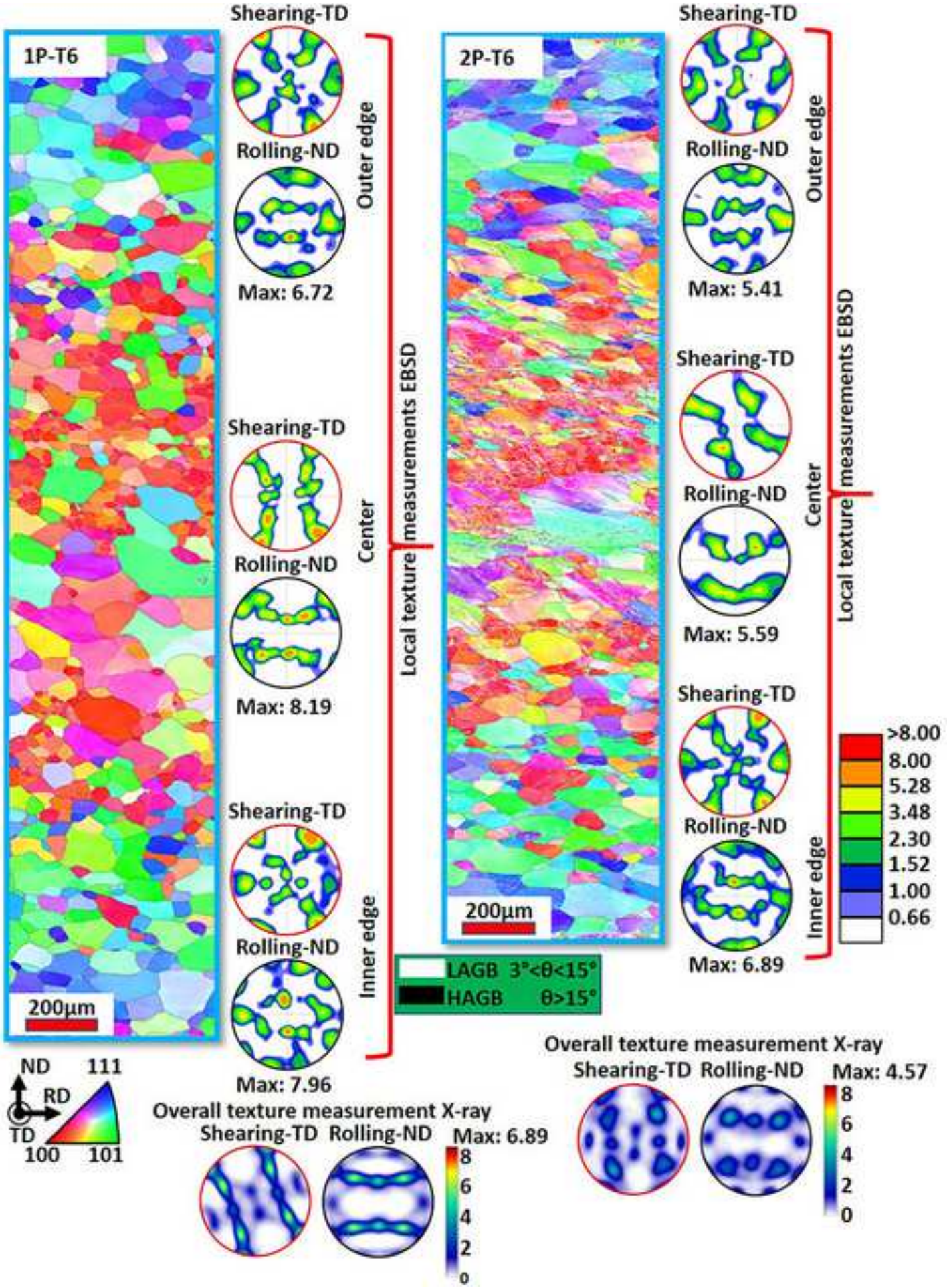

Figure7

Click here to download Figure Figure 7.jpg

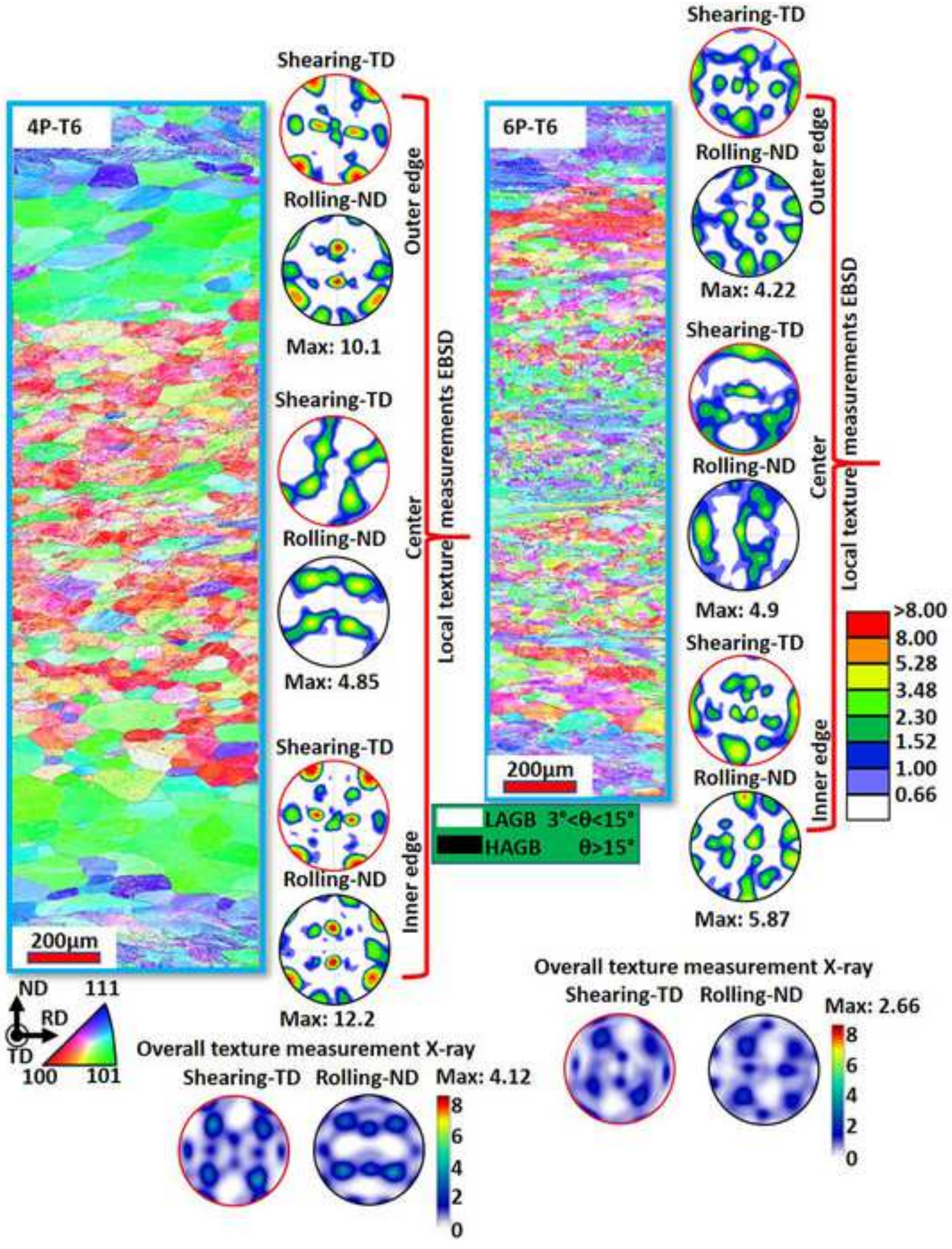

Figure8

Click here to download Figure Figure 8.jpg

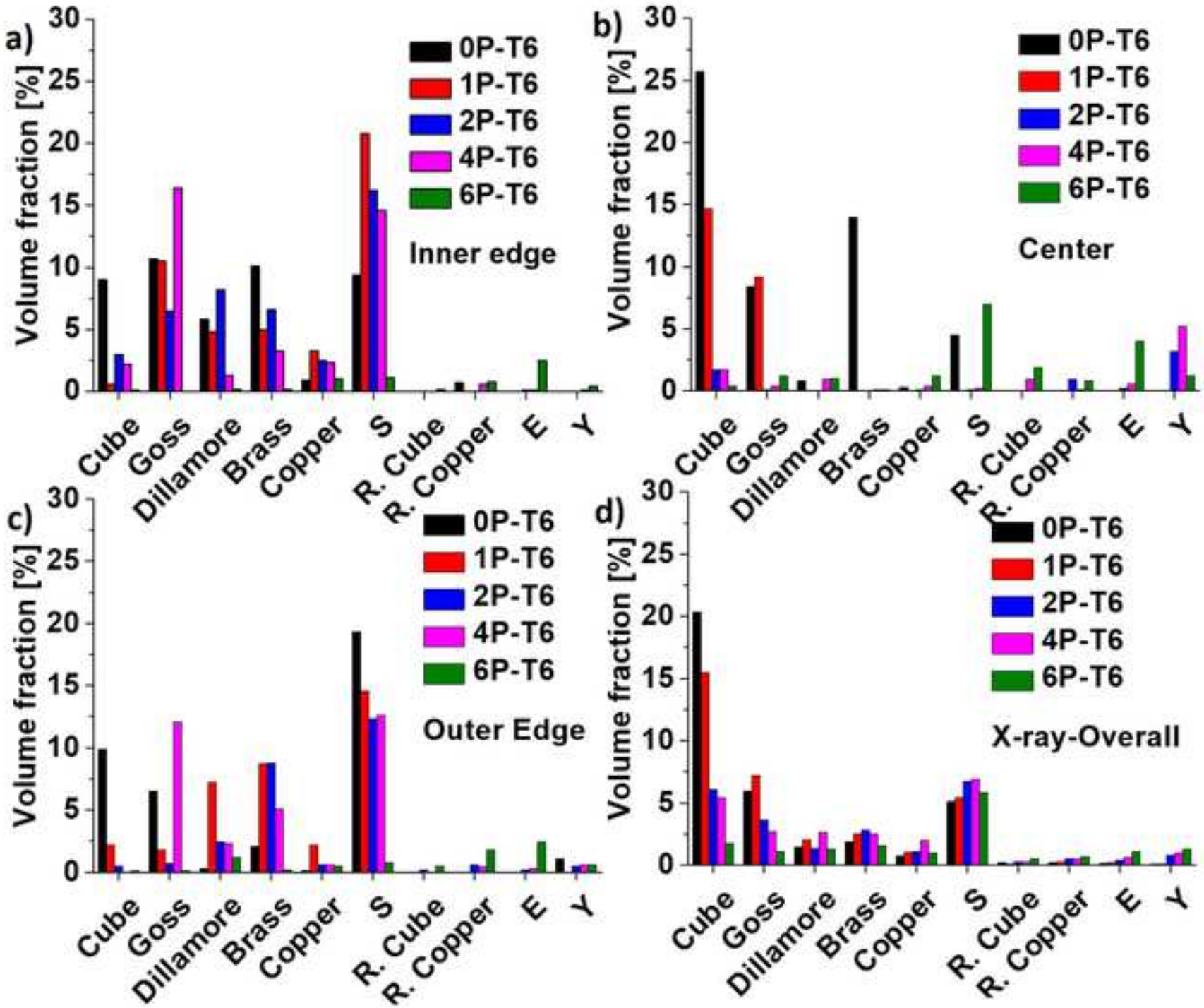

Figure9

Click here to download Figure Figure 9.jpg

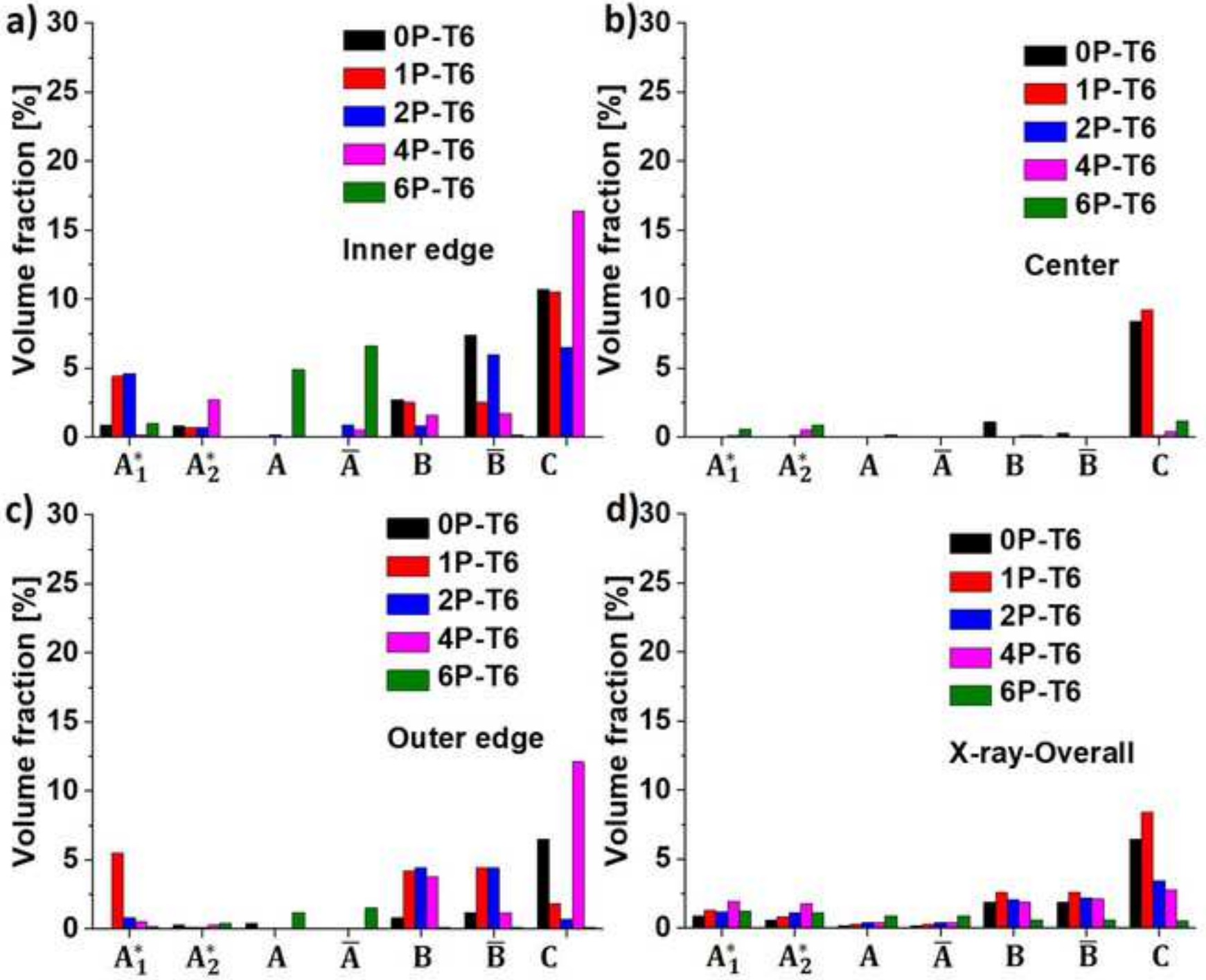

Figure10

Click here to download Figure Figure 10.jpg

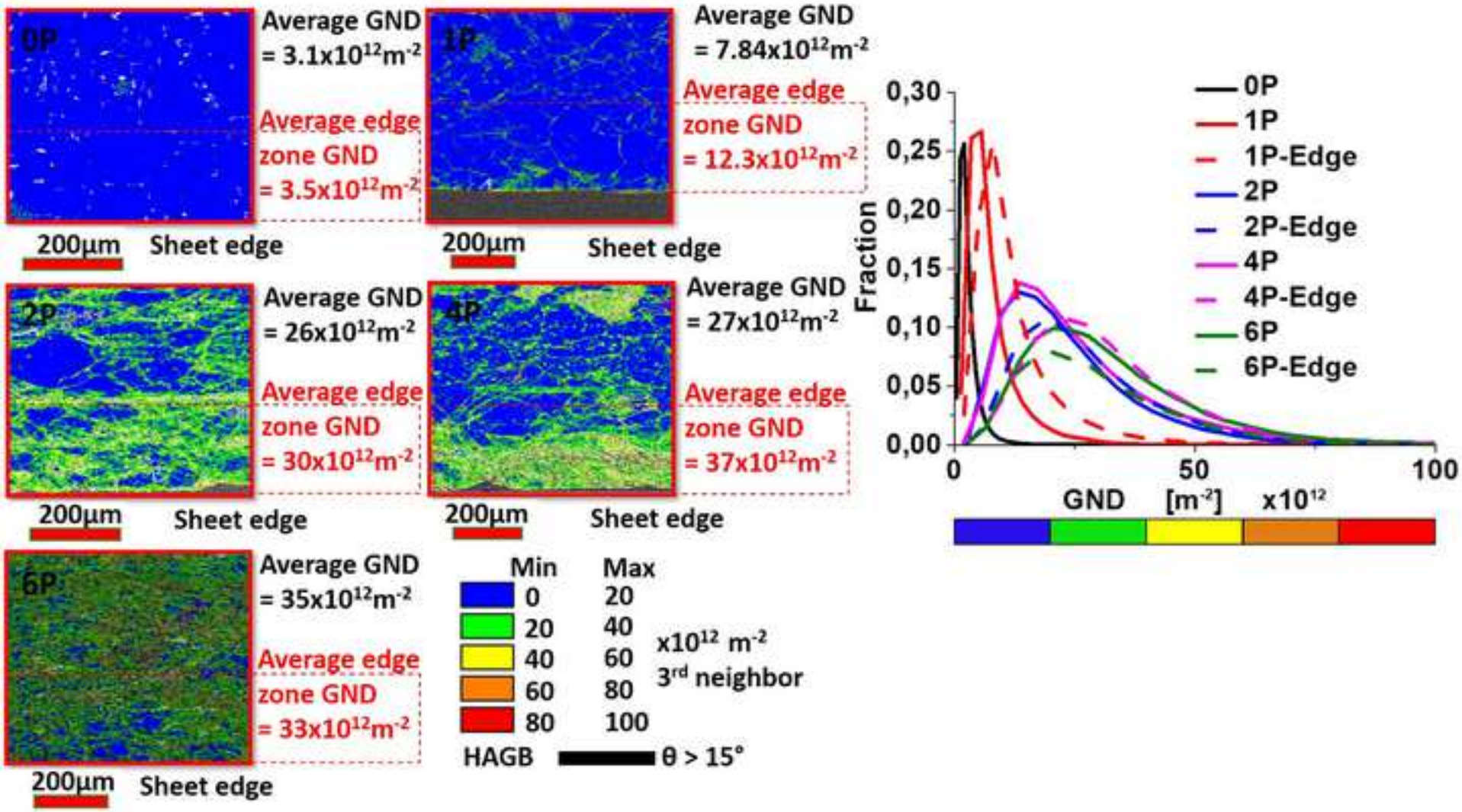

FigureS1

Click here to download Figure Figure S1.jpg

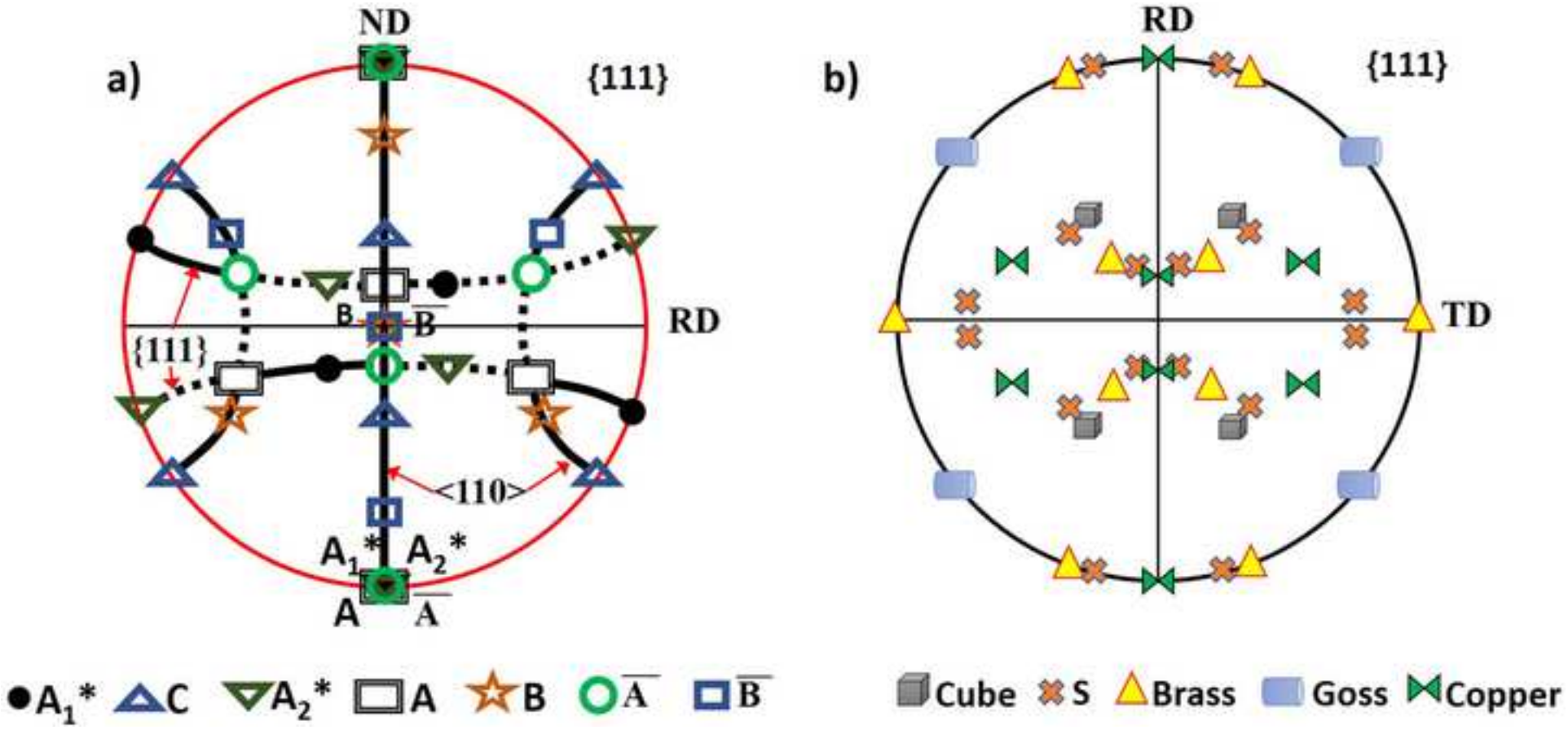

Table 1. Microstructure characteristics in the three zones.

ECASE passes	Average misorientation [°] Inner, center and outer edges			Grain size [µm] Inner, center and outer edges			HAGB [%] Inner, center and outer edges		
0	22.2	15.8	23.1	39.5	30.9	39.5	63.0	43.0	62.0
1	12.8	14.7	16.0	32.3	28.8	31.3	48.1	46.9	58.6
2	10.6	9.1	8.7	25.4	12.7	17.4	29.7	16.6	20.7
4	11.0	11.8	10.0	10.1	7.8	14.5	17.5	14.5	18.9
6	10.2	11.5	12.0	8.7	5.8	10.6	16.7	24.2	16.7

Table S2. Ideal texture components for FCC materials.

Texture component	Miller indices	Euler angles		
	{hkl}<uvw>	φ_1	ϕ	φ_2
Cube	{001}<100>	0	0	0
Rotated cube[a]	{001}<110>	45	0	0
Goss	{011}<100>	0	45	0
Rotated goss	{011}<011>	90	45	0
Goss twin	{113}<332>	90	25	45
Brass	{011}<211>	35	45	0
Goss/brass	{011}<115>	16	45	0
A	{011}<111>	55	45	0
Y[a]	{111}<112>	90	55	45
E[a]	{111}<011>	60	55	45
Copper	{112}<111>	90	35	45
Rotated copper[a]	{112}<011>	0	35	45
Copper twin	{554}<115>	90	74	45
Dillamor[a]	{4411}<11118>	90	27	45
S	{123}<634>	59	37	63
S/brass	{414}<234>	49	40	75

[a]Shearing texture components

Table S3. Simple shear texture components

Texture component	Miller indices	Euler angles		
	{hkl}<uvw>	φ_1	Φ	φ_2
A_1*	{111}<112>	35.26/215.26	45	0
		125.26	90	45
A_2*	{111}<112>	144.74	45	0
		54.74	90	45
A	{111}<110>	0	35.26	45
$\overline{A}$	{111}<110>	180	35.26	45
B	{112}<110>	0	54.74	45
$\overline{B}$	{112}<110>	60	54.74	45
C	{001}<110>	90	45	0